Shape-Dependent Catalysis

DOI: 10.1002/anie.200603961

# Near-Monodisperse Tetrahedral Rhodium Nanoparticles on Charcoal: The Shape-Dependent Catalytic Hydrogenation of Arenes**

*Kang Hyun Park, Kwonho Jang, Hae Jin Kim, and Seung Uk Son**

Transition metals loaded on charcoal are useful reagents for a wide variety of organic transformations. Moreover, these heterogeneous systems are promising industrial catalysts. For example, commercially available Pd/C is frequently used in debenzylation, hydrogenation, and C–C bond-formation reactions in the laboratory and is also used in industry,[1] and Ni/C,[2] Cu/C,[3] and Co/C[4] have recently been developed as catalysts for coupling, hydrosilylation, and cycloaddition reactions, respectively.

Commercially available Rh/C shows excellent catalytic activity in a broad range of organic reactions, including hydrogenation, hydroformylation, hydrocarbonylation, and reductive coupling of aryl halides,[5] and considerable effort has been aimed at enhancing the efficiency of this reagent. For instance, better solid supports, such as nanoporous carbon and layered clays, have been developed.[6] Recently, the Wai and Koningsberger groups have shown that carbon nanotubes and nanofibers are better supports owing to their enhanced dispersion ability.[7] An ionic liquid has also been used as a promising support for rhodium; the resulting complex showed good stability and catalytic activity in the hydrogenation of benzene.[8]

Other research has focused on the size- and shape-control of rhodium-metal particles. There has been significant progress in reducing their size to obtain a larger surface area, and a wide variety of synthetic routes that lead to spherical rhodium nanoparticles are known.[9] However, shape-control to form other types of rhodium nanoparticles has been little explored.

Recently, there has been a great deal of interest in the shape-dependent physical and chemical properties of nanocrystals. The El-Sayed group, for example, described the shape-dependent catalytic activity of platinum nanocrystals in electron-transfer reactions. They reported that tetrahedral Pt nanocrystals are more active than spherical or cubic ones because they contain more catalytically active atoms on the surface.[10] The groups of Somorjai and Tilley have reported the synthesis of cubic and flower-like rhodium nanoparticles.[11] However, to our knowledge, there are no reports on tetrahedral rhodium nanoparticles. Herein we report the preparation of tetrahedral Rh nanoparticles loaded on charcoal by an organometallic approach along with their excellent catalytic activity in the hydrogenation of arenes.

Low-temperature, kinetically controlled synthesis is one of the most common strategies for the shape evolution of nanoparticles because the reactivity of each crystal plane can be differentiated efficiently under these conditions.[12] The key strategy in this study is based on the use of relatively unstable compounds **1**–**3** as precursors for the formation of nanocrystals at low temperature.

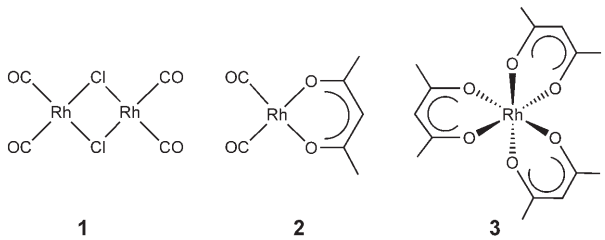


**1** **2** **3**

In a typical synthesis, compound **1** was added to well-dried oleylamine and the temperature was increased gradually to 170 °C. The color of the solution changed from red to black during this process. The reaction mixture was stirred for one hour at this temperature and then poured into methanol to form a black precipitate, which was separated by centrifugation (see Supporting Information for details). The TEM images of these black powders show the presence of (4.9 ± 0.4)-nm-sized, near-monodisperse tetrahedral nanoparticles (Figure 1a and Supporting Information). The catalytically active (111) lattice planes are mainly observed in the HR-TEM images, which also indicate the high crystallinity of the synthesized nanoparticles (inset of Figure 1a) When the reaction temperature was decreased to 130 °C, (2.8 ± 0.3)-nm-sized tetrahedral nanoparticles were obtained, which suggests the incomplete consumption of the precursors. The powder X-ray diffraction (XRD) and electron diffraction (ED) patterns of the tetrahedral nanoparticles were indexed to the (111), (200), (220), and (311) lattice planes of cubic rhodium (JSPDS no. 5-685; see Supporting Information).

We also prepared spherical nanoparticles to compare the shape-dependent catalytic activity of both types of nanoparticles. The surfactants surrounding the surface of nano-

[*] Dr. K. H. Park, K. Jang, Prof. S. U. Son
Department of Chemistry
Sungkyunkwan University
Suwon 440-746 (Korea)
Fax: (+82) 31-299-4572
E-mail: sson@skku.edu
Homepage: http://chem.skku.ac.kr/~sson
Dr. H. J. Kim
Korea Basic Science Institute
Daejeon 350-333 (Korea)

[**] This work was supported by the Hydrogen Energy R&D Center, a 21st century Frontier R&D Program funded by the Ministry of Science and Technology of Korea. K.H.P. is grateful for a grant from the Korea Research Foundation (MOEHRD) (KRF-2005-005J11901).

Supporting Information for this article is available on the WWW under http://www.angewandte.org or from the author.

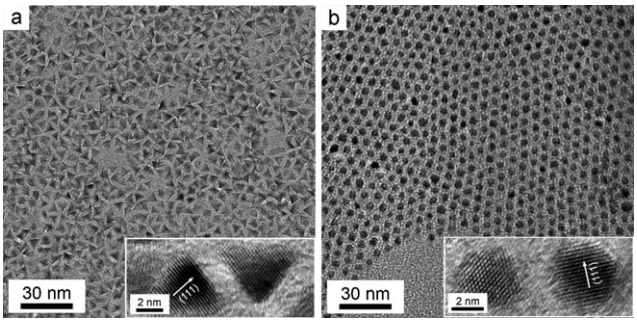


***Figure 1.*** Low-magnification TEM and HR-TEM images (insets) of (4.9 ± 0.4)-nm tetrahedral (a) and (4.8 ± 0.4)-nm spherical (b) Rh nanoparticles prepared from precursors **1** and **3**, respectively (see Supporting Information for size-distribution diagrams).

particles need to be considered as it was reported recently that surfactants have a significant influence on the catalytic activity of nanoparticles by changing the chemical environment of the surface atoms.[13] Therefore, only oleylamine was used as a surfactant so as to normalize the effect of the surfactant on the catalysis. It is believed that spherical nanoparticles are thermodynamically favorable for synthesis,[10b] therefore harsher conditions were used with precursor **1**. As the reaction temperature is increased to 190 °C, the tetrahedral nanoparticles appear to coalesce to form larger, sphere-like nanoparticles (size (6.4 ± 0.6) nm; Figure 2 d). Figure 2 a shows the dimerization of the tetrahedral nanoparticles through the (111) lattice plane. Polycrystalline and almost single-crystalline sphere-like nanoparticles can be observed in the HR-TEM images shown in Figures 2 b and c. When the reaction temperature is increased to 235 °C, approximately half of the nanoparticles present are spherical with a diameter of (9.5 ± 1.0) nm. However, there is still a significant portion of tetrahedral nanoparticles. When precursor **1** is rapidly injected into hot oleylamine at 235 °C, the tetrahedral nanoparticles disappear completely and irregularly shaped polydisperse nanoparticles are formed. These observations imply that spherical nanoparticles are thermodynamically more favorable. We therefore turned our attention to other precursors that are more stable than **1**.

A mixture of tetrahedral and spherical nanoparticles is formed when precursor **2** is heated at 190 °C. The proportion of spherical nanoparticles is higher than with precursor **1** (Figure 2 e). However, there is still a significant proportion of tetrahedral nanoparticles present. Moreover, the size distribution, (5.1 ± 0.9) nm, becomes broad at a temperature of 235 °C, therefore the more stable precursor **3** was used instead. When the reaction temperature is slowly increased to 235 °C, irregularly shaped nanoparticles with a large size distribution, (4.1 ± 0.8) nm, are obtained. However, when a solution of precursor **3** is rapidly injected into hot oleylamine at 220 °C, rectangular nanoparticles with a size distribution of (9.3 ± 2.6) nm are mainly observed (Figure 2 f). Interestingly, no tetrahedral nanoparticles are found. The HR-TEM image of these rectangular nanoparticles mainly shows the less catalytically active (200) lattice plane (Figure 2 g). Spherical nanoparticles with a somewhat broad size distribution, (5.0 ± 0.6) nm, begin to form at 235 °C (Figure 2 h). This observation suggests that the rectangle is a metastable shape in the process

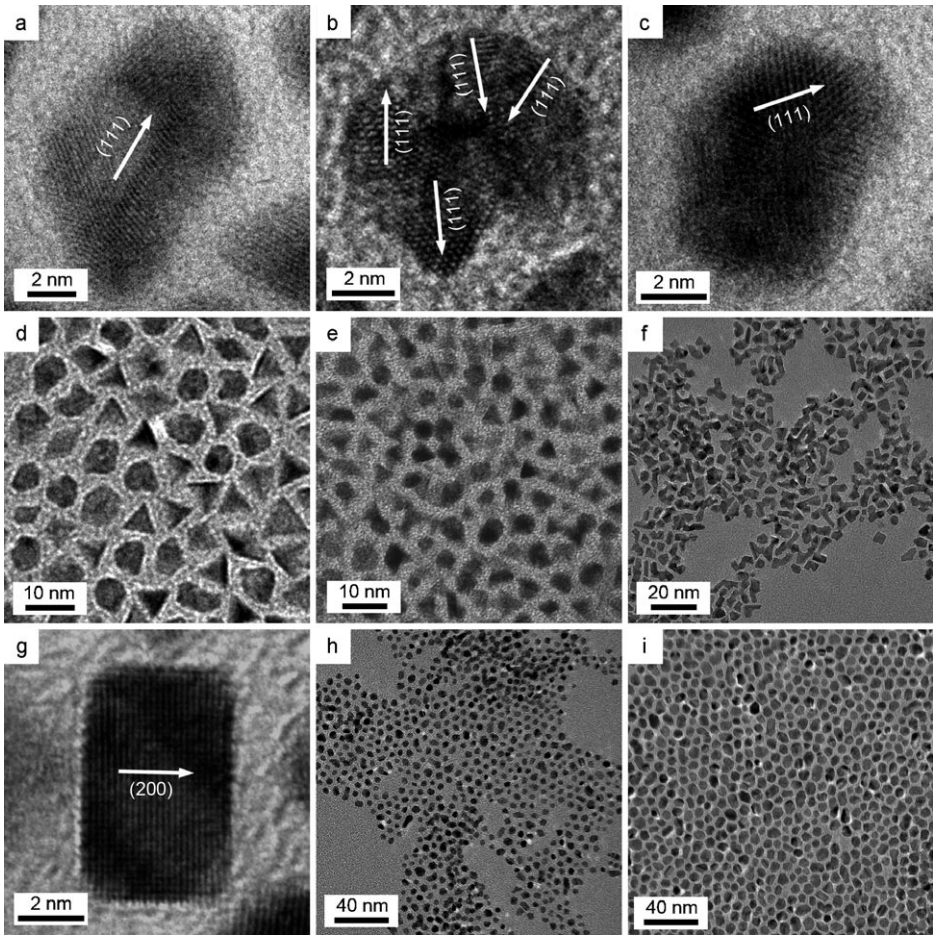


***Figure 2.*** Selected HR-TEM images (a–c) of the particles in (d) and normal TEM images of the mixture of tetrahedral and spherical Rh nanoparticles (d) formed at 190 °C from precursor **1**; e) the mixture of tetrahedral and spherical particles formed at 190 °C from precursor **2**; f) a TEM image of rectangular rhodium nanoparticles formed at 220 °C by injection of precursor **3** into the hot solution and g) an HR-TEM image for one of the nanoparticles in (f); h) a TEM image of polydisperse spherical nanoparticles formed at 235 °C from precursor **3** and i) (7.1 ± 0.7)-nm spherical nanoparticles formed at 250 °C from the double concentration of precursor **3**.

of forming spherical particles. Highly crystalline and monodisperse spherical nanoparticles with a size distribution of (4.8 ± 0.4) nm are obtained at 250 °C (Figure 1b). Similar to the tetrahedral nanoparticles, the HR-TEM images of these spherical nanoparticles mainly show the catalytically active (111) lattice plane. The size of these spherical nanoparticles can be controlled by changing the amount of precursor **3**. For example, particles with a size distribution of (7.1 ± 0.7) nm are formed when the precursor concentration was doubled (Figure 2i).

The chemical environment of the surface atoms is a key factor that determines the catalytic activity and selectivity of these nanoparticles. Coordinatively unsaturated metal atoms on the corners or edges in nanocrystals are crucial for the catalytic activity of particles. The (111) faces are the most catalytically active in cubic phase nanoparticles and the (100) faces are the least active.[10] It has been reported that tetrahedral Pt nanoparticles have entirely (111) faces on the surface and spherical nanoparticles have both (111) and (100) faces.[10] Moreover, the atoms on the corners or edges of 4.8-nm, tetrahedral Pt nanoparticles comprise 28% of the total number of atoms and 35% of the surface atoms. In contrast, the atoms on the corner or edges of 4.9-nm, almost-spherical Pt nanoparticles comprise 3% of the total atoms and 13% of the surface atoms. There is a recent report on the synthesis of rhodium nanocubes.[11] From the viewpoint of catalytic applications, the surface of a cube is known to show the catalytically less active (100) faces.[10a,11] As Rh nanoparticles have the same space group (*Fm3m*) as Pt metal, it is expected that tetrahedral rhodium nanoparticles should be the most promising for use as a heterogeneous catalyst.

The catalytic activities of tetrahedral and spherical nanoparticles were compared by immobilizing colloidal nanoparticles on activated charcoal. The nanoparticles were deposited by refluxing dispersed colloidal nanoparticles with dried activated charcoal in methanol. The absolute amount of rhodium metal on the charcoal was determined by inductively coupled plasma atomic emission spectroscopy (ICP-AES). The hydrogenation of arenes was chosen as a model reaction because it is a simple but industrially very important reaction.[14] Initially, the catalytic activity for the hydrogenation of anthracene was tested because both the activity and selectivity can be determined. Three main products are formed in the hydrogenation of anthracenes:[7a] those produced by hydrogenation of the central ring (**B**), the two side rings (**D**), or only one side ring (**C**). Table 1 and Figure 3 summarize the results. As expected, tetrahedral Rh nanoparticles on charcoal show excellent activity and selectivity in this reaction, catalyzing hydrogenation far more efficiently than either spherical or commercial Rh/C catalysts.

Monitoring the reaction by gas chromatography revealed that the first hydrogenation is complete to form products **B** and **C** within 10 min under 1 atm of $H_2$ at room temperature, whereas it takes two hours to convert **C** into **D**. It appears that tetrahedral nanoparticles are 5.8-times (Figure 3 and Table 1, entry 2 vs. entry 3) and 109-times (Figure 3 and Table 1, entry 2 vs. entry 5) more active than spherical nanoparticles and commercial Rh/C, respectively. Interestingly, the selectivity (hydrogenation of the central ring vs. side rings (**B**:(**C**+**D**)) of tetrahedral rhodium nanoparticles (1:49; entry 2, Table 1) is much higher than those of spherical nanoparticles (1:14; entry 3, Table 1) and commercial Rh/C (1:1.8; entry 5, Table 1). The selectivity of tetrahedral nanoparticles is higher (up to 1:142; entry 1, Table 1) under a pressure of 10 atm of $H_2$, and that of commercial Rh/C increases to 1:15 (entry 4, Table 1). Tetrahedral rhodium nanoparticles on charcoal are therefore more active and selective in the hydrogenation of anthracene.

***Table 1:*** Comparison of catalytic activities and selectivities of Rh on charcoal for the hydrogenation of anthracene.[a]

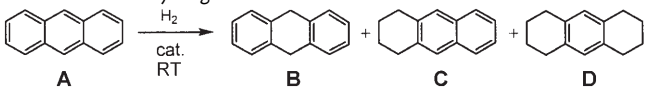


| Entry | Cat.[b] | *P* [atm] | *t* [h] | Conv.[c] [%] | Selectivity [%] B | C | D |
|---|---|---|---|---|---|---|---|
| 1 | ▲/C | 10 | 0.5 | 100 | 0.7 | 0.0 | 99.3 |
| 2 | ▲/C | 1 | 2 | 100 | 2.0 | 0.0 | 98.0 |
| 3 | ●/C | 1 | 2 | 99.5 | 6.7 | 76.3 | 17.0 |
| 4 | Rh/C | 10 | 0.5 | 57.3 | 6.4 | 81.0 | 12.6 |
| 5 | Rh/C | 1 | 2 | 4.8 | 35.4 | 45.8 | 18.8 |

[a] Reaction conditions: 1.00 mmol of anthracene and 1 mol% of Rh/C (based on ICP analysis) in methanol at room temperature. [b] (4.9 ± 0.4)-nm tetrahedral rhodium nanoparticles on charcoal (▲/C), (4.8 ± 0.4)-nm spherical rhodium nanoparticles on charcoal (●/C), and commercial Rh/C. [c] Conversion determined by GC-MS.

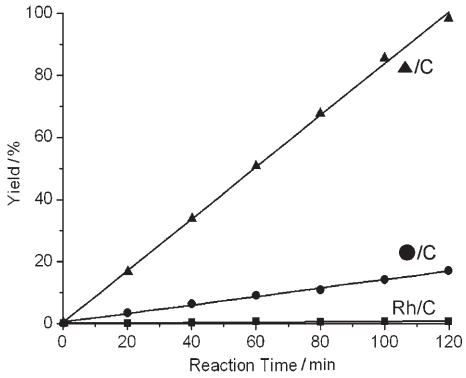


***Figure 3.*** A comparison of the catalytic activities of tetrahedral (▲) and spherical Rh nanoparticles on charcoal (●) and commercial Rh/C catalysts for the formation of **D**. See Supporting Information for selectivity data for **D** and conversion of substrate.

A recent review has highlighted that a high activity is not necessarily indicative of a low selectivity in many reactions.[15] Many other factors related to the activity and selectivity of heterogeneous catalysts have been discussed. In particular, the fact that the atoms on different faces of nanocrystals have different reaction kinetics and preferences in chemical reactions has been studied experimentally by molecular-beam-based methods.[16]

An iodine poisoning experiment showed that the reaction occurs in a heterogeneous manner (see Supporting Information).

The next set of experiments was aimed at screening a range of substrates. The reactions shown in Table 2 were

  

***Table 2:*** Hydrogenation of arenes in the presence of tetrahedral rhodium nanoparticles on charcoal.[a]

| Entry | Substrate | Product | $t$ [h] | Conv.[b] [%] | TOF[c] [$h^{-1}$] |
|---|---|---|---|---|---|
| 1 | anisole | methyl cyclohexyl ether | 1 | 100 | 300 |
| 2[d] | anisole | methyl cyclohexyl ether | 1 | 100 | 300 |
| 3 | benzene | cyclohexane | 0.5 | 100 | 600 |
| 4 | toluene | methylcyclohexane | 0.5 | 100 | 600 |
| 5 | phenol | cyclohexanol | 1 | 100 | 300 |
| 6 | methyl benzoate | methyl cyclohexane-carboxylate | 0.5 | 100 | 600 |
| 7 | naphthalene | octahydronaphthalene | 2 | 100 | 250 |
| 8 | diphenylmethane | dicyclohexylmethane | 2 | 83 | 249 |
| 9 | diphenylmethane | dicyclohexylmethane | 3 | 100 | 200 |
| 10 | diphenyl ether | oxydicyclohexane | 1.5 | 50 | 200 |
| 11[e] | diphenyl ether | oxydicyclohexane | 2.5 | 100 | 224 |

[a] Reaction conditions: 1.00 mmol of substrate and 1 mol% of tetrahedral rhodium nanoparticles on charcoal (based on ICP analysis) in methanol at room temperature under 1 atm of $H_2$. [b] Determined by GC-MS. [c] TOF = turnover frequency defined as mol of $H_2$ consumed per mol of total metal per hour. [d] The catalyst recovered from entry 1 was used. [e] Cyclohexanol (13%) was detected as a by-product. The formation of cyclohexane could not be ascertained by GC-MS.

monitored by GC-MS. As expected, the tetrahedral rhodium nanoparticles on charcoal show excellent activity with a wide range of arenes. The hydrogenation of monoarenes, for example, is complete within one hour (entries 1, 3–6 in Table 2). ICP-AES analysis of the reaction mixture after the hydrogenation of anisole showed no loss of rhodium metal and the recovered catalysts showed the same catalytic activity, as shown by comparing entries 1 and 2 in Table 2. Naphthalene and diphenylmethane were hydrogenated cleanly after two and three hours, respectively. In the case of diphenyl ether the reactant had been consumed after 2.5 h; in this reaction, cyclohexanol was formed as a by-product (13%).

In conclusion, near-monodisperse tetrahedral rhodium nanoparticles have been successfully prepared by an organometallic approach. High-quality spherical rhodium nanoparticles have also been synthesized for comparison by a hot-injection method. The $(4.9 \pm 0.4)$-nm tetrahedral rhodium nanoparticles on charcoal show 5.8- and 109-times higher activity for the hydrogenation of anthracene than spherical nanoparticles and commercial Rh/C, respectively. Moreover, the tetrahedral nanoparticles show excellent activity with a range of arenes. We believe that the development of more active Rh/C catalysts by taking advantage of the shape-control of metal particles will have a large impact on organic synthesis and industry.

Received: September 27, 2006
Revised: October 23, 2006
Published online: December 21, 2006

**Keywords:** heterogeneous catalysis · hydrogenation · nanoparticles · rhodium · supported catalysts

[1] For recent examples see: a) C. R. LeBlond, A. T. Andrews, J. R. Sowa, Jr., Y. Sun, *Org. Lett.* **2001**, *3*, 1555; b) H. Sakurai, T. Tsukuda, T. Hirao, *J. Org. Chem.* **2002**, *67*, 2721; c) Y. Mori, M. Seki, *J. Org. Chem.* **2003**, *68*, 1571.
[2] B. H. Lipshutz, *Adv. Synth. Catal.* **2001**, *343*, 313.
[3] B. H. Lipshutz, B. A. Frieman, A. E. Tomaso, Jr., *Angew. Chem.* **2006**, *118*, 1281; *Angew. Chem. Int. Ed.* **2006**, *45*, 1259.
[4] S. U. Son, S. I. Lee, Y. K. Chung, *Angew. Chem.* **2000**, *112*, 4318; *Angew. Chem. Int. Ed.* **2000**, *39*, 4158.
[5] a) P. N. Rylander, *Hydrogenation Methods*, Academic Press, New York, **1985**; b) W. M. Pearlman, *Org. Synth. Coll.* **1973**, *5*, 670; c) M. Fujita, T. Hiyama, *Org. Synth. Coll.* **1993**, *8*, 16; d) A. Akao, K. Sato, N. Nonoyama, T. Mase, N. Yasuda, *Tetrahedron Lett.* **2006**, *47*, 969.
[6] a) G. Vitulli, C. Evangelisti, P. Pertici, A. M. Caporusso, N. Panziera, P. Salvadori, M. G. Faga, C. Manfredotti, G. Martra, S. Coluccia, A. Balerna, S. Colonna, S. Mobilio, *J. Organomet. Chem.* **2003**, *681*, 37; b) M. Fuchs, B. Jenewein, S. Penner, K. Hayek, G. Rupprechter, D. Wang, R. Schlögl, J. J. Calvino, S. Bernal, *Appl. Catal. A* **2005**, *294*, 279.
[7] a) B. Yoon, C. M. Wai, *J. Am. Chem. Soc.* **2005**, *127*, 17174; b) T. G. Ros, D. E. Keller, A. J. van Dillen, J. W. Geus, D. C. Koningsberger, *J. Catal.* **2002**, *211*, 85.
[8] a) M. A. Gelesky, A. P. Umpierre, G. Machado, R. R. B. Correia, W. C. Magno, J. Morais, G. Ebeling, J. Dupont, *J. Am. Chem. Soc.* **2005**, *127*, 4588; b) X. Mu, J. Meng, Z. Li, Y. Kou, *J. Am. Chem. Soc.* **2005**, *127*, 9694; c) G. S. Fonseca, A. P. Umpierre, P. F. P. Fichtner, S. R. Teixeira, J. Dupont, *Chem. Eur. J.* **2003**, *9*, 3263.
[9] a) J. Schulz, S. Levigne, A. Roucoux, H. Patin, *Adv. Synth. Catal.* **2002**, *344*, 266; b) J.-L. Pellegatta, C. Blandy, V. Collière, R. Choukroun, B. Chaudret, P. Cheng, K. Philippot, *J. Mol. Catal. A* **2002**, *178*, 55; c) M. Harada, D. Abe, Y. Kimura, *J. Colloid Interface Sci.* **2005**, *292*, 113; d) A. J. Bruss, M. A. Gelesky, G. Machado, J. Dupont, *J. Mol. Catal. A* **2006**, *252*, 212.
[10] a) R. Narayanan, M. A. El-Sayed, *Nano Lett.* **2004**, *4*, 1343; b) R. Narayanan, M. A. El-Sayed, *J. Am. Chem. Soc.* **2004**, *126*, 7194.
[11] J. D. Hoefelmeyer, K. Niesz, G. A. Somorjai, T. D. Tilley, *Nano Lett.* **2005**, *5*, 435.
[12] N. Pradhan, H. Xu, X. Peng, *Nano Lett.* **2006**, *6*, 720.
[13] a) C. A. Stowell, B. A. Korgel, *Nano Lett.* **2005**, *5*, 1203; b) S. Jansat, M. Gómez, K. Philippot, G. Muller, E. Guiu, C. Claver, S. Castillón, B. Chaudret, *J. Am. Chem. Soc.* **2004**, *126*, 1592; c) M. Tamura, H. Fujihara, *J. Am. Chem. Soc.* **2003**, *125*, 15742.
[14] a) V. Mévellec, A. Nowicki, A. Roucoux, C. Dujardin, P. Granger, E. Payen, K. Philippot, *New J. Chem.* **2006**, *30*, 1214; b) G. S. Fonseca, E. T. Silveira, M. A. Gelesky, J. Dupont, *Adv. Synth. Catal.* **2005**, *347*, 847; c) I. S. Park, M. S. Kwon, N. Kim, J. S. Lee, K. Y. Kang, J. Park, *Chem. Commun.* **2005**, 5667; d) A. Roucoux, J. Schulz, H. Patin, *Adv. Synth. Catal.* **2003**, *345*, 222.
[15] H. Mayr, A. R. Ofial, *Angew. Chem.* **2006**, *118*, 1876; *Angew. Chem. Int. Ed.* **2006**, *45*, 1844.
[16] J. Libuda, *ChemPhysChem.* **2004**, *5*, 625.

  